



Published in final edited form as:

J Stroke Cerebrovasc Dis. 2017 April ; 26(4): 779–786. doi:10.1016/j.jstrokecerebrovasdis.2016.10.017.

White Matter Hyperintensity Associations with Cerebral Blood Flow in Elder Subjects Stratified by Cerebrovascular Risk

Ahmed A Bahrani, MS^{1,2}, David K Powell, PhD³, Guoqiang Yu, PhD¹, Eleanor S Johnson, BS³, Gregory A Jicha, MD, PhD⁴, and Charles D Smith, MD^{1,3,4}

¹Department of Biomedical Engineering, School of Engineering, University of Kentucky

²Department of Biomedical Engineering, AL-Khwarizmi College of Engineering, University of Baghdad, Baghdad, Iraq

³Magnetic Resonance Imaging and Spectroscopy Center (MRISC), University of Kentucky

⁴Department of Neurology, University of Kentucky Medical College

Abstract

Goal—Add clarity to the relationship between deep and periventricular brain white matter hyperintensities, cerebral blood flow and cerebrovascular risk in older persons.

Methods—Deep and periventricular WMH and regional grey and white matter blood flow from arterial spin labeling were quantified from magnetic resonance imaging scans of 26 cognitively normal elder subjects stratified by cerebrovascular disease risk. FLAIR images were acquired using a high-resolution 3D sequence that reduced partial volume effects seen with slice-based techniques.

Findings—Deep WMH (dWMH) but not periventricular WMH (pWMH) were increased in the high CVD risk patients; pWMH but not dWMH were associated with decreased regional cortical (GM) blood flow. We also found blood flow in white matter is decreased in regions of both pWMH and dWMH, with a greater degree of decrease in pWMH areas.

Conclusion—WMH are usefully divided into dWMH and pWMH regions because they demonstrate differential effects. Three-dimensional regional WMH volume is a potentially valuable marker for CVD based on associations with cortical CBF and with white matter CBF.

Keywords

white matter hyperintensities; small vessel disease; cerebral blood flow; arterial spin labeling image; segmentation; fluid attenuated inversion recovery; vascular risk

Correspondence: Charles D Smith, MD, Magnetic Resonance Imaging and Spectroscopy Center (MRISC)Room 62, MRISC (Davis-Mills) Building Chandler Medical Center, 740 South Limestone Street, Lexington, KY 40536-0098, Phone : 859-323-1113, FAX: 859-323-1068.

Publisher's Disclaimer: This is a PDF file of an unedited manuscript that has been accepted for publication. As a service to our customers we are providing this early version of the manuscript. The manuscript will undergo copyediting, typesetting, and review of the resulting proof before it is published in its final citable form. Please note that during the production process errors may be discovered which could affect the content, and all legal disclaimers that apply to the journal pertain.

Introduction

Cerebrovascular disease (CVD) is a common medical morbidity in the United States, with high rates of disability through stroke and dementia [1, 2]. Detection and characterization of existing cerebrovascular disease, therefore, remains an important medical issue. An understudied aspect of cerebrovascular disease is the relationship between cerebral blood flow (CBF) and white matter hyperintensities (WMH, [3, 4]). WMH are periventricular and deep regions of abnormal signal commonly seen on MRI scans of elderly and high vascular risk patients [5, 6]. It has been found that WMH embody an ischemic component with functional consequences including cognitive decline and dementia, but due to the underlying complexity of these lesions a full formulation of their significance has not been achieved [7, 8]. In this study we analyzed the relationship between WMH and CBF in subjects stratified by cerebrovascular risk. The aim of this study was to find relationships between WMH, CBF and CVD risk, expecting that WMH would increase with increased CVD risk and with decreased CBF.

Materials and Methods

Subjects

Twenty-six healthy subjects were recruited by the Center for Clinical and Translational Science (CCTS) and the Sanders-Brown Center on Aging at the University of Kentucky. Written consent was obtained from each individual before participation according to an approved protocol from the Institutional Review Board (IRB) at the University of Kentucky.

A CVD risk score, based on Framingham risk estimation modified for stroke prediction[9], was assigned to each patient by study neurologists. The Framingham study risk score is based on several parameters, e.g., gender, age, history of diabetes, blood pressure, smoking history, and cholesterol level, and used to predict CVD over ten years for each subject. The Framingham scoring scale range is 1 – 30 points. Subjects were divided, based on their risk score, into two groups: high-risk (n = 12) and low-risk (n = 14) for CVD, based on a cutoff of 15 points. Image analysis was blind to age and CVD risk status.

MRI acquisition

A Siemens 3T TIM Trio MRI scanner at the University of Kentucky Magnetic Resonance Imaging and Spectroscopy Center (MRISC) equipped with a 32-channel head coil was used to scan subjects. Acquisition sequences were: (1) T1-weighted Magnetization-Prepared Rapid Acquisition Gradient Echo (MPRAGE), TE 2.3 ms, TR 2530 ms, IR 1100 ms, FA is 7°, 1 × 1 × 1 mm resolution full brain coverage (2) Fluid Attenuated Inversion Recovery (FLAIR), TE 388 ms, TR 6000 ms, IR is 2200 ms, 3D 1 × 1 × 1 mm with no gap between slices, and (3) Pulsed Arterial-Spin-Labeling (PASL) TE 12 ms, TR 3400 ms, IR₁ 700 ms, IR₂ 1900 ms, 4 × 4 × 4 mm resolution with 1 mm gap between slices, full brain coverage excluding the cerebellum.

Image Processing

MRI image processing used semi-automated methods to quantitate regional WMH volume and CBF flow values. These methods are summarized in Figure 1. Two images were registered and averaged to increase the signal-to-noise ratio. Scalp and bone tissue were stripped using the FSL FMRIB software library (FSL v5.0.8) Brain Extraction Tool (BET) (<http://fsl.fmrib.ox.ac.uk/fsl/fslwiki/BET>). Slice by slice cleanup of unwanted tissue was performed using the Medical Image Processing Analysis and Visualization (MIPAV v7.2.0) application (<http://mipav.cit.nih.gov>). The stripped brain image was converted to a mask by thresholding (brain mask). FLAIR and PASL images were registered to the image in SPM12 (<http://www.fil.ion.ucl.ac.uk/spm>) and stripped of extraneous tissue using the brain mask.

Multimodal segmentation was performed on masked, FLAIR and ASL brain images in the SPM12 unified regime to create separate native-space images representing grey matter (GM; Figure 2A), white matter (WM) and cerebrospinal fluid (CSF) using an inhouse segmentation template created from 145 images of normal subjects. WM was modeled as two separate tissue classes to represent variations due to WM intensities [10]. The International Consortium for Brain Mapping (ICBM) atlas reference was registered to the segmentation template, and atlas regions combined to create masks representing the frontal, temporal, parietal and occipital brain regions for both GM (Figure 2B) and WM (Figure 2C).

CBF quantification

The ICBM lobar masks were registered to each subject's native-space ASL image using the inverse transform generated during segmentation. Median CBF values were extracted from each grey matter template region (Figure 2D).

White Matter Hyperintensity Quantification

The two WM segmentation images (Figures 3A and 3B) were summed (Figure 3C) and converted to a binary WM mask in native space (Figure 3D). In a few instances WM voxels were misclassified in an extraneous tissue segment, likely due to partial volume effects; in these cases, these voxels were added to the two WM segments before binary conversion. The unitary WM mask isolated WM in the FLAIR image (Figure 3E) by multiplication, (Figure 3F). The Gaussian fit to the histogram of WM voxels was used to set the threshold for WMH (Figure 3G), as the mean plus $3 \times S.D.$, corresponding to a p-value of 0.01. The threshold values were applied to each FLAIR image and 1 mm Gaussian filtered to remove noise, creating a WMH image for each subject (Figure 3H).

A final quality-control procedure used a high-contrast display of the FLAIR image at the Gaussian-fit mean center and window value of $10 \times S.D.$, side by side with the WMH image, comparing slice by slice for correspondence between isolated WMH and FLAIR hyperintensities. Manual editing of extraneous pixels due to pulsation and flow artifacts was needed occasionally, resulting in the final WMH image (Figure 3H), quantitated by calculating total voxels and total WMH voxel volume [10].

Voxels in the WMH image were divided into pWMH and dWMH using the following method designed to produce a reproducible and consistent definition of pWMH and dWMH:

(1) the CSF segment (Figure 4A) was used to generate a mask by thresholding at 0.33 (Figure 4B). Connected voxels were morphologically identified as belonging to ventricles. (Figure 4C) and isolated (Figure 4D). The ventricular volume was intensity-inverted (Figure 4E) and multiplied by the FLAIR image (Figure 4F) to exclude the CSF (Figure 4G), (2) the border of the ventricular mask was morphologically identified (Figure 4H) and dilated (5^3 voxels; Figure 4I), then multiplied by the CSF-excluded FLAIR image to identify periventricular tissue (Figure 4J). Ten percent of the mean value from periventricular tissue voxel histogram was set as minimum threshold level to obtain the periventricular binary mask (Figure 4K), and (3) this mask was multiplied by the total WMH mask (Figure 4L; cf. Figure 3H) to obtain pWMH (Figure 4M), and the negative of this periventricular binary mask multiplied by the total WMH mask to obtain dWMH (Figure 4N).

Statistical Methods

Multivariate analysis of variance (MANOVA) models used log-transformed measured WMH volumes as repeated independent variables because of their typical skewed distributions (JMP v9, SAS Institute). Dependent variables were risk group (high versus low vascular risk) and total intracranial volume (TIV) to control for head size. Post hoc contrasts of dWMH and pWMH versus risk group relationships were performed. A similar model was used for ASL cerebral blood flow in three defined WM regions: the two containing either dWMH or pWMH, and one without WMH. Age, risk group and TIV were used as covariates in this model.

To test relationships between dWMH and pWMH, a standard least squares model was constructed with log dWMH as the dependent variable, and risk group nested within log pWMH as independent variables, with TIV as control for head size. A p-value of 0.05 was considered significant; a p-value <0.10 marginally significant.

Results

The 26 subjects had a mean age of 77.8 ± 6.8 years (range 66 – 88). There were twenty-three females (mean age 77.8 ± 6.9) and three males (mean age 77.0 ± 7.9). There was a significant difference in age between risk groups: the low-risk group had a mean age of 72.7 ± 4.2 and the high-risk group had a mean age of 83 ± 4.6 ($p < 0.0001$).

White Matter Hyperintensities

Total WMH volume positively correlated with independent visual ratings using the Longstreth scale[11], confirming that volumes correspond to what a trained neurologist interprets as WMH (Figure 5A). There was a significant correlation between pWMH and dWMH in the regression model, but the relationship between pWMH and dWMH was different for high and low-risk subjects: the slope of regression was higher in the high-risk group (1.26 ± 0.22 SEM; $t = 5.5$, $p < 0.0001$) compared to low-risk (0.86 ± 0.34 , $t=2.5$, $p = 0.02$). The mean dWMH volume was higher in the high-risk group compared to low risk ($t = 2.3$, $p = 0.03$; Figure 5B).

MANOVA analysis confirmed that WMH volume was higher in the high-risk group ($F = 5.8$, $p = 0.02$). Further analysis demonstrates that dWMH volume was higher in the high-risk

group ($t = 2.2$, $p = 0.04$), but pWMH volume was not significantly different ($t = 1.0$, $p = 0.34$) between groups.

Age correlated with total WMH ($p = 0.04$) and dWMH ($p = 0.03$) but not pWMH volume ($p = 0.10$). There was a strong correlation seen between age and risk score ($r^2 = 0.56$; $p < 0.0001$).

Cerebral Blood Flow (CBF)

There were no differences in global or in regional cortical GM CBF between risk groups. There was no association between CBF and age. We analyzed associations between WMH volume and regional CBF. Results are shown in Table 1. Correlations were significant between parietal WMH volume and posterior frontal, parietal, temporal, and occipital CBF, and marginally significant with total CBF. Occipital pWMH volume was significantly correlated with CBF in the medial temporal GM (Table 1).

Average white matter CBF was calculated for three WM regions containing dWMH, pWMH or neither lesion ($F = 53.5$, $p < 0.0001$; Figure 6). Age, risk group and TIV did not significantly affect CBF. Post-hoc paired comparisons showed significantly decreased CBF in dWMH ($t = 5.7$, $p < 0.001$) and pWMH ($t = 11.0$, $p < 0.0001$) regions compared to normal appearing white matter. CBF in pWMH was less than in dWMH areas ($t = 3.1$, $p = 0.003$).

Discussion

The aim of this study was to find relationships between WMH, CBF and CVD risk in elder patients. CVD risk was assessed by the Framingham CVD stroke risk score assigned to each patient. Fourteen subjects with low-risk were compared to twelve subjects with high-risk. We used a 3-D FLAIR WMH imaging technique that improved resolution and registration, and reduced partial volume effects compared to slice-based techniques. The main findings are that dWMH but not pWMH are increased in high-risk patients, and that pWMH but not dWMH are associated with decreased regional cortical (GM) blood flow. We also found blood flow in white matter is decreased in regions of both pWMH and dWMH, with a greater degree of decrease in pWMH areas.

The underlying origin of WMH remains controversial, perhaps because different mechanisms responsible for their appearance and pathologies can be found at autopsy that so far are not distinguishable using current MRI methods[2, 7, 12–18]. The strongest and most consistent associations with WMH are age and certain cerebrovascular risk factors including diabetes, hypertension, hypercholesterolemia, and cigarette smoking[8, 9, 19–26]. These factors are included in vascular risk measures such as the Framingham score used in this study. A genetic component may be involved in cases where evidence of CVD is lacking[27–31].

Age associations with WMH are likely explained by the accumulation of vascular disease over time together with other changes in cerebral white matter that may be unrelated to small vessel cerebrovascular disease *per se*, such as cerebral amyloid angiopathy or AD-

related changes[32, 33]. Nonetheless, WMH are taken with much supporting evidence to represent a marker of classical small vessel cerebrovascular disease in white matter. Small vessel CVD is increasingly recognized as an important pathological contributor to clinical decline in our aging US population, showing strong associations with both gait disorders and vascular dementia [34–36]. Vascular dementia can occur as a pure form, or often together with more common dementias including Alzheimer’s disease (where it is termed mixed vascular dementia)[37].

We divided WMH into dWMH and pWMH for several reasons[10, 38–42]. Firstly, the white matter tracts adjacent to the ventricles encompassed by pWMH are limbic (cingulum) and motor (corticospinal and related tracts), whereas dWMH are more likely to involve long association tracts and thus long-range inter-regional connectivity. The possibility that clinical correlates of dWMH and pWMH may be different is also supported by the association of dWMH but not pWMH with vascular dementia [10, 43]. Finally, the small-vessel circulation in white matter may be different between deep and periventricular zones, with a greater vulnerability of the periventricular region to large- vessel disease [44]. This is consistent with our finding that low cortical CBF is associated with greater pWMH.

We found that the relationship between pWMH and dWMH was different depending on risk group: the increase in dWMH per given change in pWMH was higher in the high-risk group, even though pWMH volume was the same. This suggests that vascular risk factors are associated with more widespread small vessel disease in white matter, whether directly or indirectly via large vessel flow compromise. Other evidence of small vessel disease in our data was decreased white matter CBF in both dWMH and pWMH regions. However, these differences were not related to age or to CVD risk status.

There are several caveats to the interpretation of our data. The first is the association of age with risk status in our patients. Age is strongly associated with CVD, but there may be other independent effects of age on WMH we aren’t able to discern in our analysis. Better selection of subjects and larger recruitment would have helped overcome this limitation. Another caution is the relatively low proportion of patients with high grades of WMH. We were able to offset this problem by normalizing distributions of WMH and using non-parametric correlations for CBF, still achieving significant results, but these findings should be confirmed in future studies. Additional methodologic analysis considerations include our planned use of a 3D ASL acquisition for better comparison with 3D WMH volumes.

Conclusions

We find evidence that WMH are usefully divided into dWMH and pWMH regions because they demonstrate differential associations with CVD and demographic risk factors. 3D WMH volume is a potentially valuable marker for CVD that is able to differentiate associations of pWMH and dWMH with risk factor profiles as well as cortical and white matter CBF. Further studies using such methods in distinct and larger cohorts are needed to conform and extend the present findings.

Acknowledgments

We wish to thank The Higher Committee for Education Development in Iraq for their support, assistance from Weikai Kong, Yu Shang, Chong Huang, and Abner Rayapati, and the help we received from the University of Kentucky Alzheimers Center, particularly from Dr Fred Schmitt of the ADC. This study was supported by a pilot award (GY) from the National Institutes of Health (NIH) P30 #AG028383 and a Grant-In-Aid (GY) from the American Heart Association (AHA) #16GRNT30820006.

This study was supported by a pilot award (GY) from the National Institutes of Health (NIH) P30 #AG028383 and a Grant-In-Aid (GY) from the American Heart Association (AHA) #16GRNT30820006

References

1. Go AS, Mozaffarian D, Roger VL, Benjamin EJ, Berry JD, Baha MJ, et al. Heart disease and stroke statistics—2014 update: a report from the American Heart Association. *Circulation*. 2014; 129:e28–e292. [PubMed: 24352519]
2. Jellinger KA. The pathology of ischemic-vascular dementia: an update. *Journal of the neurological sciences*. 2002;203–204. 153–7.
3. Brickman AM, Zahra A, Muraskin J, Steffener J, Holland CM, Habeck C, et al. Reduction in cerebral blood flow in areas appearing as white matter hyperintensities on magnetic resonance imaging. *Psychiatry research*. 2009; 172:117–20. [PubMed: 19324534]
4. Bastos-Leite AJ, Kuijper JP, Rombouts SA, Sanz-Arigita E, van Straaten EC, Gouw AA, et al. Cerebral blood flow by using pulsed arterial spin-labeling in elderly subjects with white matter hyperintensities. *AJNR American journal of neuroradiology*. 2008; 29:1296–301. [PubMed: 18451090]
5. Gootjes L, Teipel SJ, Zebuhr Y, Schwarz R, Leinsinger G, Scheltens P, et al. Regional distribution of white matter hyperintensities in vascular dementia, Alzheimer's disease and healthy aging. *Dementia and geriatric cognitive disorders*. 2004; 18:180–8. [PubMed: 15211074]
6. DeBette S, Markus HS. The clinical importance of white matter hyperintensities on brain magnetic resonance imaging: systematic review and meta-analysis. *BMJ (Clinical research ed)*. 2010; 341:c3666.
7. Raman MR, Preboske GM, Przybelski SA, Gunter JL, Senjem ML, Vemuri P, et al. Antemortem MRI findings associated with microinfarcts at autopsy. *Neurology*. 2014; 82:1951–8. [PubMed: 24793188]
8. Wardlaw JM, Allerhand M, Doubal FN, Valdes Hernandez M, Morris Z, Gow AJ, et al. Vascular risk factors, large-artery atheroma, and brain white matter hyperintensities. *Neurology*. 2014; 82:1331–8. [PubMed: 24623838]
9. D'Agostino RB, Wolf PA, Belanger AJ, Kannel WB. Stroke risk profile: adjustment for antihypertensive medication. The Framingham Study. *Stroke; a journal of cerebral circulation*. 1994; 25:40–3.
10. Smith CDJ, Eleanor S, Van Eldik Linda J, Jicha Gregory A, Schmitt Frederick A, Nelson Peter T, Kryscio Richard J, Murphy Ronan R, Wellnitz Clinton V. Peripheral (deep) but not Periventricular MRI White Matter Hyperintensities are Increased in Clinical Vascular Dementia Compared to Alzheimer's Disease. 2016
11. Longstreth WT Jr, Manolio TA, Arnold A, Burke GL, Bryan N, Jungreis CA, et al. Clinical correlates of white matter findings on cranial magnetic resonance imaging of 3301 elderly people. The Cardiovascular Health Study. *Stroke; a journal of cerebral circulation*. 1996; 27:1274–82.
12. Erten-Lyons D, Woltjer R, Kaye J, Mattek N, Dodge HH, Green S, et al. Neuropathologic basis of white matter hyperintensity accumulation with advanced age. *Neurology*. 2013; 81:977–83. [PubMed: 23935177]
13. Gouw AA, Seewann A, van der Flier WM, Barkhof F, Rozemuller AM, Scheltens P, et al. Heterogeneity of small vessel disease: a systematic review of MRI and histopathology correlations. *Journal of neurology, neurosurgery, and psychiatry*. 2011; 82:126–35.

14. Hooshmand B, Polvikoski T, Kivipelto M, Tanskanen M, Myllykangas L, Erkinjuntti T, et al. Plasma homocysteine, Alzheimer and cerebrovascular pathology: a population-based autopsy study. *Brain : a journal of neurology*. 2013; 136:2707–16. [PubMed: 23983028]
15. Jagust WJ, Zheng L, Harvey DJ, Mack WJ, Vinters HV, Weiner MW, et al. Neuropathological basis of magnetic resonance images in aging and dementia. *Annals of neurology*. 2008; 63:72–80. [PubMed: 18157909]
16. Kaur B, Himali JJ, Seshadri S, Beiser AS, Au R, McKee AC, et al. Association between neuropathology and brain volume in the Framingham Heart Study. *Alzheimer disease and associated disorders*. 2014; 28:219–25. [PubMed: 24614264]
17. Smith CD, Snowdon DA, Wang H, Markesbery WR. White matter volumes and periventricular white matter hyperintensities in aging and dementia. *Neurology*. 2000; 54:838–42. [PubMed: 10690973]
18. Smith CD, Snowdon D, Markesbery WR. Periventricular white matter hyperintensities on MRI: correlation with neuropathologic findings. *Journal of neuroimaging : official journal of the American Society of Neuroimaging*. 2000; 10:13–6. [PubMed: 10666976]
19. Abraham HM, Wolfson L, Moscufo N, Guttmann CR, Kaplan RF, White WB. Cardiovascular risk factors and small vessel disease of the brain: blood pressure, white matter lesions, and functional decline in older persons. *Journal of cerebral blood flow and metabolism : official journal of the International Society of Cerebral Blood Flow and Metabolism*. 2015
20. Gattringer T, Enzinger C, Ropele S, Gorani F, Petrovic KE, Schmidt R, et al. Vascular risk factors, white matter hyperintensities and hippocampal volume in normal elderly individuals. *Dementia and geriatric cognitive disorders*. 2012; 33:29–34. [PubMed: 22377559]
21. Jeerakathil T, Wolf PA, Beiser A, Massaro J, Seshadri S, D'Agostino RB, et al. Stroke risk profile predicts white matter hyperintensity volume: the Framingham Study. *Stroke; a journal of cerebral circulation*. 2004; 35:1857–61.
22. Miwa K, Tanaka M, Okazaki S, Yagita Y, Sakaguchi M, Mochizuki H, et al. Multiple or mixed cerebral microbleeds and dementia in patients with vascular risk factors. *Neurology*. 2014; 83:646–53. [PubMed: 25015364]
23. Rostrup E, Gouw AA, Vrenken H, van Straaten EC, Ropele S, Pantoni L, et al. The spatial distribution of age-related white matter changes as a function of vascular risk factors—results from the LADIS study. *NeuroImage*. 2012; 60:1597–607. [PubMed: 22305990]
24. Vuorinen M, Spulber G, Damangir S, Niskanen E, Ngandu T, Soininen H, et al. Midlife CAIDE dementia risk score and dementia-related brain changes up to 30 years later on magnetic resonance imaging. *J Alzheimers Dis*. 2015; 44:93–101. [PubMed: 25190628]
25. Wang R, Fratiglioni L, Laukka EJ, Lovden M, Kalpouzos G, Keller L, et al. Effects of vascular risk factors and APOE epsilon4 on white matter integrity and cognitive decline. *Neurology*. 2015; 84:1128–35. [PubMed: 25672924]
26. Wang R, Fratiglioni L, Laveskog A, Kalpouzos G, Ehrenkrona CH, Zhang Y, et al. Do cardiovascular risk factors explain the link between white matter hyperintensities and brain volumes in old age? A population-based study. *European journal of neurology : the official journal of the European Federation of Neurological Societies*. 2014; 21:1076–82.
27. Adib-Samii P, Devan W, Traylor M, Lanfranconi S, Zhang CR, Cloonan L, et al. Genetic architecture of white matter hyperintensities differs in hypertensive and nonhypertensive ischemic stroke. *Stroke; a journal of cerebral circulation*. 2015; 46:348–53.
28. Adib-Samii P, Rost N, Traylor M, Devan W, Biffi A, Lanfranconi S, et al. 17q25 Locus is associated with white matter hyperintensity volume in ischemic stroke, but not with lacunar stroke status. *Stroke; a journal of cerebral circulation*. 2013; 44:1609–15.
29. Carmelli D, DeCarli C, Swan GE, Jack LM, Reed T, Wolf PA, et al. Evidence for genetic variance in white matter hyperintensity volume in normal elderly male twins. *Stroke; a journal of cerebral circulation*. 1998; 29:1177–81.
30. Haffner C, Malik R, Dichgans M. Genetic factors in cerebral small vessel disease and their impact on stroke and dementia. *Journal of cerebral blood flow and metabolism : official journal of the International Society of Cerebral Blood Flow and Metabolism*. 2015

31. Lin Q, Huang WQ, Tzeng CM. Genetic associations of leukoaraiosis indicate pathophysiological mechanisms in white matter lesions etiology. *Reviews in the neurosciences*. 2015; 26:343–58. [PubMed: 25781674]
32. Gurol ME, Viswanathan A, Gidicsin C, Hedden T, Martinez-Ramirez S, Dumas A, et al. Cerebral amyloid angiopathy burden associated with leukoaraiosis: a positron emission tomography/magnetic resonance imaging study. *Annals of neurology*. 2013; 73:529–36. [PubMed: 23424091]
33. Lo RY, Jagust WJ. Vascular burden and Alzheimer disease pathologic progression. *Neurology*. 2012; 79:1349–55. [PubMed: 22972646]
34. Kalaria RN, Erkinjuntti T. Small vessel disease and subcortical vascular dementia. *J Clin Neurol*. 2006; 2:1–11. [PubMed: 20396480]
35. Baezner H, Blahak C, Poggesi A, Pantoni L, Inzitari D, Chabriat H, et al. Association of gait and balance disorders with age-related white matter changes: the LADIS study. *Neurology*. 2008; 70:935–42. [PubMed: 18347315]
36. van Norden AG, de Laat KF, Gons RA, van Uden IW, van Dijk EJ, van Oudheusden LJ, et al. Causes and consequences of cerebral small vessel disease. The RUN DMC study: a prospective cohort study. Study rationale and protocol. *BMC Neurol*. 2011; 11:29. [PubMed: 21356112]
37. Kalaria RN. Vascular basis for brain degeneration: faltering controls and risk factors for dementia. *Nutr Rev*. 2010; 68(Suppl 2):S74–87. [PubMed: 21091952]
38. Blahak C, Baezner H, Pantoni L, Poggesi A, Chabriat H, Erkinjuntti T, et al. Deep frontal and periventricular age related white matter changes but not basal ganglia and infratentorial hyperintensities are associated with falls: cross sectional results from the LADIS study. *Journal of neurology, neurosurgery, and psychiatry*. 2009; 80:608–13.
39. Kee Hyung P, Lee JY, Na DL, Kim SY, Cheong HK, Moon SY, et al. Different associations of periventricular and deep white matter lesions with cognition, neuropsychiatric symptoms, and daily activities in dementia. *J Geriatr Psychiatry Neurol*. 2011; 24:84–90. [PubMed: 21546648]
40. Krishnan MS, O'Brien JT, Firbank MJ, Pantoni L, Carlucci G, Erkinjuntti T, et al. Relationship between periventricular and deep white matter lesions and depressive symptoms in older people. The LADIS Study. *International journal of geriatric psychiatry*. 2006; 21:983–9. [PubMed: 16955428]
41. Noh Y, Lee Y, Seo SW, Jeong JH, Choi SH, Back JH, et al. A new classification system for ischemia using a combination of deep and periventricular white matter hyperintensities. *Journal of stroke and cerebrovascular diseases : the official journal of National Stroke Association*. 2014; 23:636–42. [PubMed: 23867045]
42. Soriano-Raya JJ, Miralbell J, Lopez-Cancio E, Bargallo N, Arenillas JF, Barrios M, et al. Deep versus periventricular white matter lesions and cognitive function in a community sample of middle-aged participants. *Journal of the International Neuropsychological Society : JINS*. 2012; 18:874–85. [PubMed: 22687604]
43. Spilt A, Goekoop R, Westendorp RG, Blauw GJ, de Craen AJ, van Buchem MA. Not all age-related white matter hyperintensities are the same: a magnetization transfer imaging study. *AJNR American journal of neuroradiology*. 2006; 27:1964–8. [PubMed: 17032876]
44. De Reuck J. The human periventricular arterial blood supply and the anatomy of cerebral infarctions. *European neurology*. 1971; 5:321–34. [PubMed: 5141149]

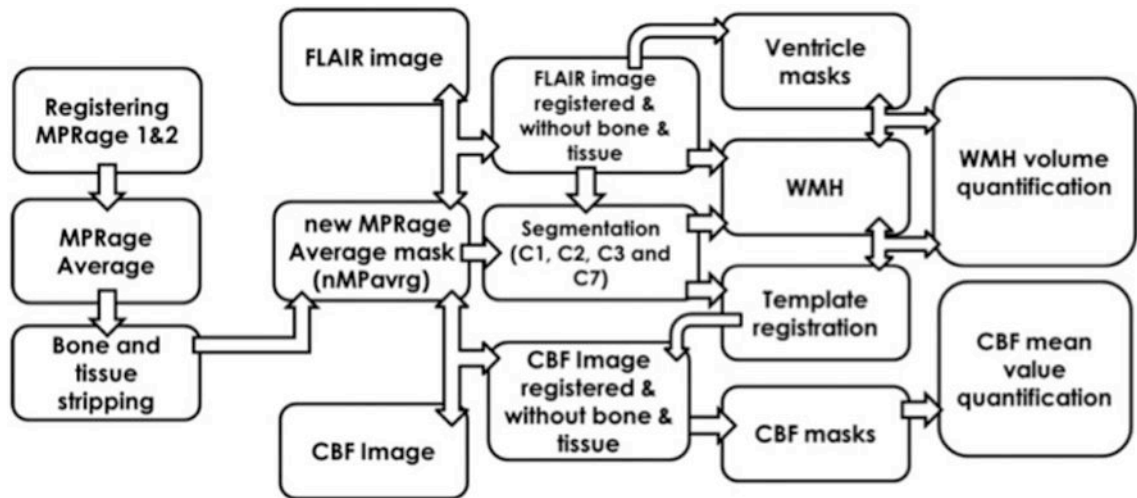


Figure 1. Diagrammatic overview of the processing workflow for quantitating WMH and CBF using, FLAIR and ASL images. Segments: C1: GM; C2: WM tissue class 1; C3: CSF; C7: WM tissue class 2.

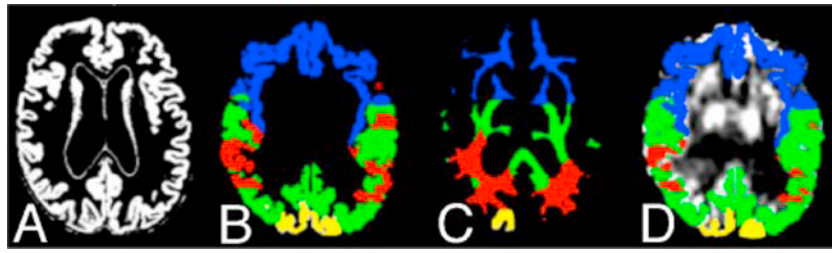


Figure 2.

A. Native-space GM segmented image. Panels B and C show ICBM template masks of WM and GM transferred to the standard space of the subject (compare with Panel A). Panel D shows the grey matter template masks applied to the registered ASL image.

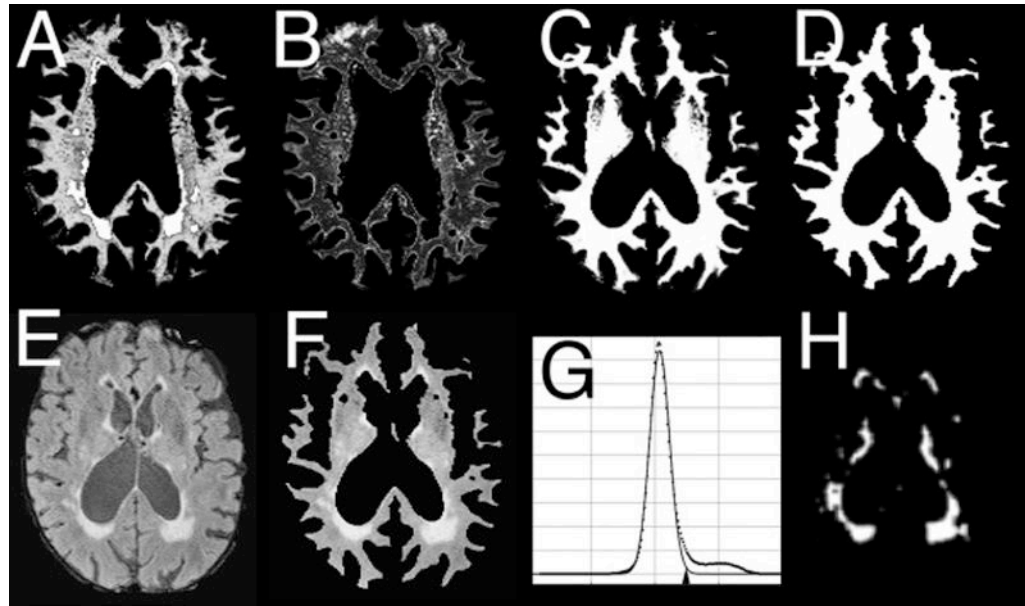


Figure 3.

Sequential steps of the segmentation process to quantitate WMH. A, B: segmented images representing two tissue classes of WM; C: total WM (A+B); D: WM mask from thresholding of D; E: FLAIR image; F: FLAIR image masked by D (FLAIR WM voxels); G: histogram of E showing Gaussian-fit and threshold of 3.0 S.D. (arrowhead); H: WMH image obtained by applying threshold to F.

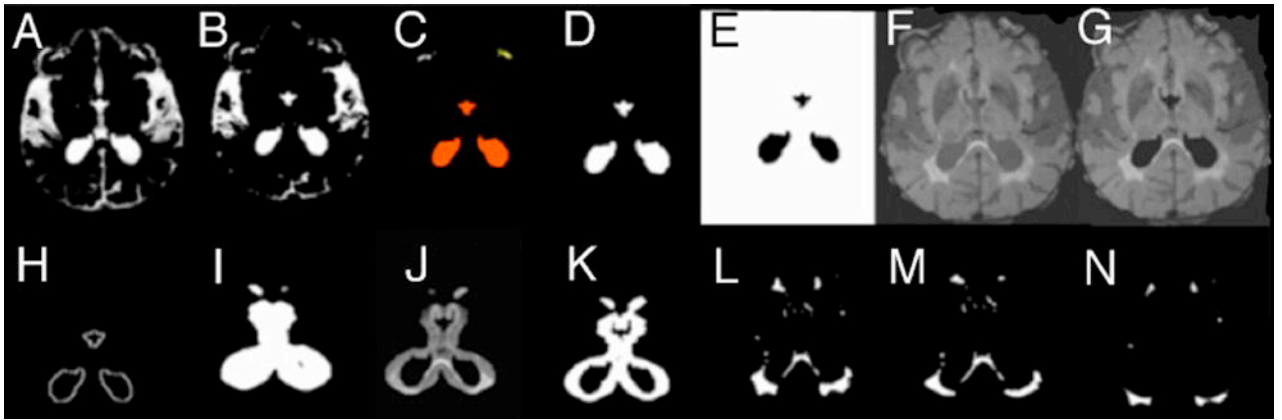


Figure 4.

Sequential steps of obtaining deep WM and pre-ventricular WM binary masks. A – the CSF isolated from other tissue, panel B. C – identifying tissue. D – ventricular tissue voxels. E – reversing the intensity of (D) and multiply by FLAIR image, F, to remove the CSF, image G. H – is the edge of (D) that is dilated by $5 \times 5 \times 5$ voxels, image I. (I and G) are multiplied to get the periventricular tissue, J, which is converted to binary image, K. L, WMH image, multiply by (K) once and the reverse intensity of (K) once to get pWMH and dWMH respectively images M and N.

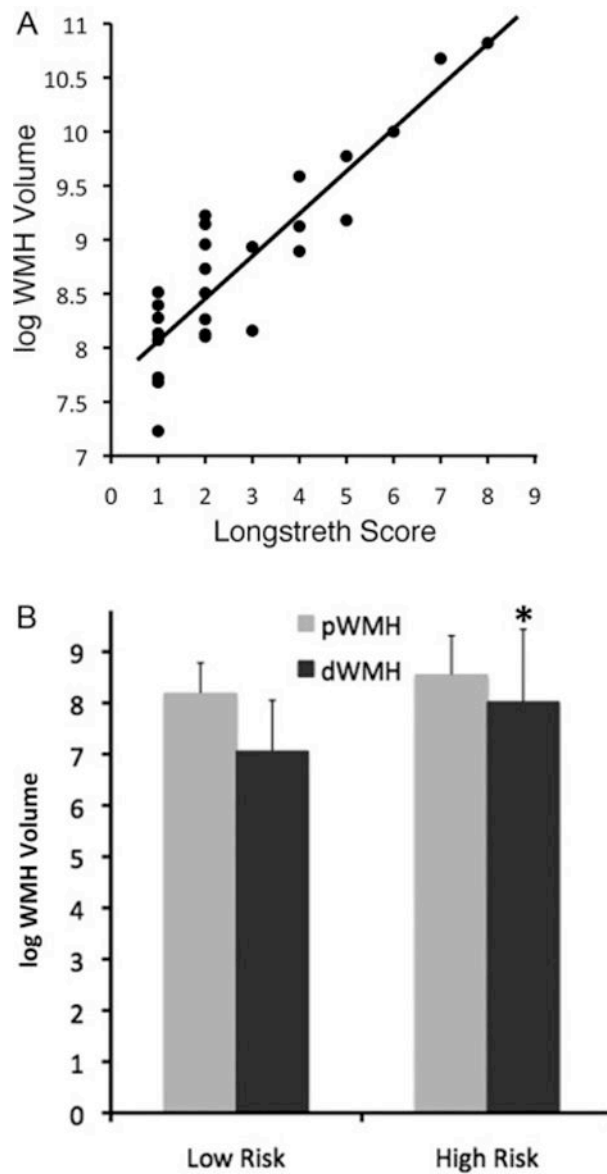


Figure 5.

(A) Linear regression of Longstreth visual rating scale (0–9) for all patients on log WMH total volume, demonstrating face validity of the WMH volume measurement (adjusted $r^2=0.88$, $p<0.0001$), (B) log WMH volume in low and high risk groups; overall volume is higher in high-risk patients ($p=0.02$), but only the dWMH volume is significant ($p = 0.04$; error bars = SD, asterisk *).

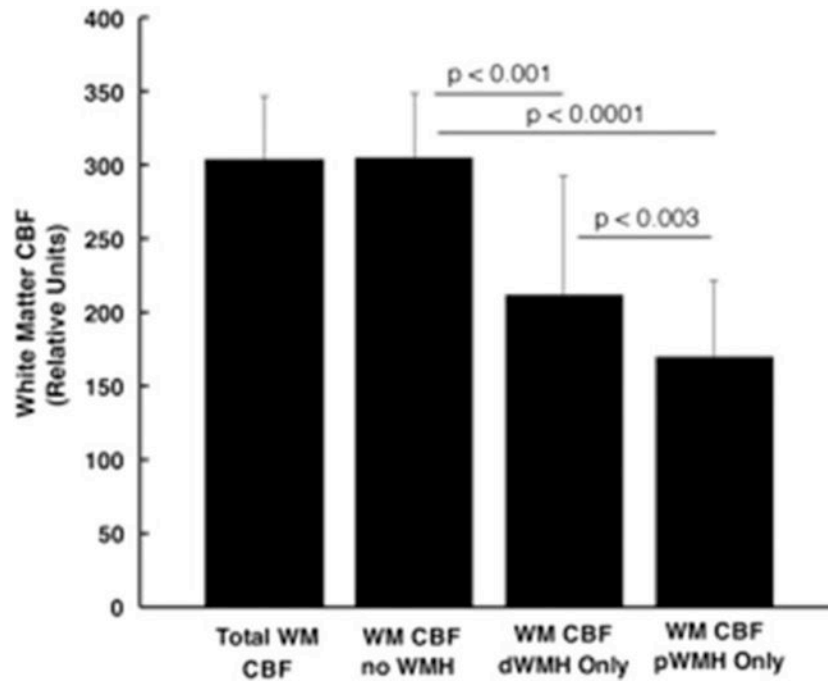


Figure 6.

ASL blood flow in white matter in order left to right: total WM including WMH, total WM but excluding WMH, dWMH regions, and pWMH regions. Paired comparisons are significantly different as shown. Lowest CBF is in pWMH regions. Bar height: mean CBF; error bars: standard deviation.

Spearman rank correlations for the pWMH and CBF for different brain regions. There were no significant correlations between dWMH or total WMH volumes with CBF.

Table 1

	Total	Frontal (ant)	Frontal (post)	Occipital	Parietal	Temporal	Temporal (medial)
WMH							
Total	-0.28 (0.15)	-0.16 (0.41)	-0.33 (0.09)	-0.37 (0.06)	-0.37 (0.06)	-0.37 (0.06)	-0.31 (0.11)
Frontal	-0.16 (0.41)	-0.16 (0.41)	-0.24 (0.23)	-0.21 (0.29)	-0.17 (0.37)	-0.23 (0.23)	-0.25 (0.20)
Occipital	-0.06 (0.73)	0.13 (0.50)	-0.006 (0.97)	-0.08 (0.66)	-0.07 (0.72)	-0.25 (0.19)	-0.42 (0.03) [§]
Parietal	-0.34 (0.08)	-0.28 (0.15)	-0.39 (0.04) [§]	-0.39 (0.04) [§]	-0.44 (0.02) [§]	-0.38 (0.05) [§]	-0.30 (0.13)
Temporal	-0.13 (0.49)	0.004 (0.98)	-0.09 (0.63)	-0.23 (0.24)	-0.18 (0.36)	-0.23 (0.24)	-0.29 (0.14)

[§] denotes significant p-value.